HHS Public Access

Author manuscript

Biochem Biophys Res Commun. Author manuscript; available in PMC 2024 February 19.

Published in final edited form as:

Biochem Biophys Res Commun. 2023 February 19; 645: 164–172. doi:10.1016/j.bbrc.2023.01.032.

MATR3 P154S knock-in mice do not exhibit motor, muscle or neuropathologic features of ALS

Marissa Dominick[1], **Nicole Houchins**[1], **Vinisha Venugopal**[1], **Aamir R. Zuberi**[2], **Cathleen M. Lutz**[2], **Bessie Meechooveet**[3], **Kendall Van Keuren-Jensen**[3], **Robert Bowser**[1], **David X. Medina**[1]

[1]Department of Translational Neuroscience, Barrow Neurological Institute, Phoenix, AZ 85013 USA

[2]Rare and Orphan Disease Translational Center, The Jackson Laboratory, Bar Harbor, ME USA

[3]Neurogenomics Division, Translational Genomics Research Institute, Phoenix, AZ USA

Abstract

Matrin 3 is a nuclear matrix protein that has many roles in RNA processing including splicing and transport of mRNA. Many missense mutations in the Matrin 3 gene (MATR3) have been linked to familial forms of amyotrophic lateral sclerosis (ALS) and distal myopathy. However, the exact role of MATR3 mutations in ALS and myopathy pathogenesis is not understood. To demonstrate a role of MATR3 mutations *in vivo*, we generated a novel CRISPR/Cas9 mediated knock-in mouse model harboring the MATR3 P154S mutation expressed under the control of the endogenous promoter. The P154S variant of the MATR3 gene has been linked to familial forms of ALS. Heterozygous and homozygous MATR3 P154S knock-in mice did not develop progressive motor deficits compared to wild-type mice. In addition, ALS-like pathology did not develop in nervous or muscle tissue in either heterozygous or homozygous mice. Our results suggest that the MATR3 P154S variant is not sufficient to produce ALS-like pathology *in vivo*.

Keywords

ALS; Matrin 3; Mouse Model; MATR3 P154S mutation; Neuropathology

Introduction:

Amyotrophic lateral sclerosis (ALS) is the most common adult-onset motor neuron disease affecting an estimated 5000 newly diagnosed patients in the US per year. Unfortunately, few options are available for ALS treatment and the three US approved drugs, Riluzole,

Declaration of interests

The authors declare that they have no known competing financial interests or personal relationships that could have appeared to influence the work reported in this paper.

Edaravone and Relyvrio, slow progression on average by only several months [1,2]. ALS is characterized by progressive loss of upper and lower motor neurons, which leads to loss of motor functions including limb weakness, swallowing, speaking, and respiration. To date, there have been over 40 causative or disease-modifying genes have been identified, and the vast majority of ALS cases (>90%) are considered sporadic [3]. Several cellular mechanisms are proposed to be involved in ALS pathogenesis such as altered RNA metabolism, nucleocytoplasmic transport defects, axonal transport defects, and excitotoxicity.

ALS and frontotemporal lobar degeneration (FTD) causing mutations in MATR3 were first reported by Johnson and colleagues in 4 different pedigrees, representing the S85C, F115C, P154S, and T622A MATR3 mutations. The S85C mutation was previously reported to cause autosomal dominant, distal-asymmetrical myopathy, but that classification was later changed to ALS [4–6]. Subsequently, a total of 13 MATR3 missense mutations have been identified and linked to ALS [7–11]. Like several other genes linked to ALS, MATR3 encodes an RNA-binding protein, further supporting a role for RNA metabolism and transport in ALS pathogenesis. Matrin 3 is a highly conserved nuclear matrix protein (98.5% between human and mouse) proposed to function in binding and stabilizing mRNAs, modulating DNA damage response, and anchoring Ato-I edited RNA within the nucleus [12–14]. Since disease causing mutations in Matrin 3 do not significantly alter its subcellular distribution [15], how these mutations induce neurodegeneration is unknown. Missense mutations in matrin 3 protein are predicted to influence its interactions with other proteins [16,17]; however, the *in vivo* functional consequences of these missense mutations are largely unknown. Matrin 3 protein has been shown to interact with both TDP-43 and FUS proteins, which are also involved in ALS pathology and mutations in either gene cause familial forms of ALS [18–20]. Importantly, Matrin 3 pathology has been demonstrated in both familial and sporadic ALS without MATR3 mutations [21,22]. This suggests that Matrin 3 may contribute to the pathogenesis of both familial and sporadic forms of ALS. Thus, studies aiming to understand Matrin 3 function and dysregulation very likely have implications in both familial and sporadic forms of ALS.

Here, we explore the neuropathology and altered functional mechanisms induced by the MATR3 P154S mutation that was previously linked to ALS [18]. To determine the role of MATR3 mutations in disease pathogenesis, we generated a novel knock-in mouse model using CRISPR/Cas9 to introduce the MATR3 P154S mutation in the endogenous murine gene. This MATR3 mutation was previously shown to alter interactions with members of the TRanscriptionEXport (TREX) complex and trafficking of FUS and TDP-43 RNAs out of the nucleus [23]. Further, this mutation has also been demonstrated to induce toxicity in yeast and primary rodent cortical neurons [24,25]. We established 2 independent lines of MATR3 P154S knock-in mice from heterozygous ($Matr3^{P154S/+}$) breeding pairs. Longitudinal assessment of motor function demonstrated that the MATR3 P154S mutation did not induce an ALS/myopathy like phenotype in heterozygous or homozygous mice. Further, neuropathological analysis likewise demonstrated no changes in markers of neurodegeneration or myopathy. Our findings further provide insight into the *in vivo* roles of MATR3 mutations, and suggest that the P154S mutation is not sufficient to produce an ALS-like phenotype in mice.

Material and Methods

Generation of MATR3 P154S mutant mice:

The MATR3 P154S mutant mouse was generated by CRISPR/Cas9 targeting of endogenous *Matr3* exon 2 of the C57BL/6J inbred mouse strain (JR 664) by co-injection of a guide RNA 5'-TCTCTACCATAACTCAATGT-3', Cas9, and a 127-nt oligonucleotide donor DNA containing the CCT>TCT nucleotide change that would convert the proline at amino acid 154 to a serine amino acid (P154S). Additionally, the donor oligonucleotide also contained a GGC>GGA nucleotide change that would preserve the incorporation of a glycine amino acid at position 153 of the protein (G153G) but would eliminate the PAM cutting site to prevent guide + Cas9 re-cutting at the target sequence. Several founders containing the desired G153G, P154S allele were generated and confirmed by DNA sequencing. Founders were mated to C57BL/6J and N1 progeny that were genomic DNA sequenced confirmed as being heterozygous for the desired G153G, P154S mutation from one of the founders were further backcrossed to C57BL/6J for additional expansion. These strains were designated JR32054 and JR32055 by the Jackson Laboratory. Subsequent mating of heterozygous mice established that the G153G, P154S mutant allele did not affect the viability or fecundity of homozygous mice, and that the numbers of wild-type, heterozygous and homozygous mutant mice generated conformed to Mendelian expectations. **Genotyping:** MATR3 P154S heterozygous male and female mice were crossed to obtain wild-type, P154S heterozygous, and P154S homozygous mice (genotypes herein referred to $Matr3^{+/+}$, $Matr3^{P154S/+}$, and $Matr3^{P154S/P154S}$, respectively). Genotyping was performed on tail biopsy DNA taken from mice at weaning. DNA was extracted using Proteinase K overnight digestion. Purified DNA was amplified using specifically designed forward (CTTCTTCCCATAATTTGCAGTC) and reverse primers (AGTTATGCGAGGTCTCACCAA) (Integrated DNA Technologies), dNTPs (New England Biolabs), and Phusion Hot Start II High Fidelity DNA Polymerase (ThermoFisher Scientific). Restriction enzyme digestion was performed using HaeIII (New England Biolabs, R0108S) to digest the wild-type GGCC sequence.

Husbandry and monitoring of health decline and motor impairment:

All procedures were approved by the Institutional Animal Care and Use Committee of the Barrow Neurological Institute/St. Joseph's Hospital and Medical Center. Mice were housed in the Barrow/St. Joseph's Hospital vivarium, accredited by the Association for Assessment and Accreditation of Laboratory Animal Care International (AAALAC). Mice were kept at a 12-hour dark/light cycle with ad libitum access to food and water. Starting at 3 weeks of age, the body weight of all mice was measured monthly. As health declined, mice were weighed and inspected weekly to daily.

Behavioral assays:

Behavioral assays were conducted on different days with at least one overnight rest between different assays. Mice were moved to the behavior testing facility 30 minutes prior to commencing any assay to allow the animals to acclimate to the new testing environment. Rotarod (Panlab, Harvard Apparatus) is an automated apparatus that measures motor coordination, balance and motor learning ability. Mice are placed on an accelerating rod starting at 4 rpm and accelerating to 40 rpm over 300s. The latency is measured as the

cumulative time (s) the subject maintains its balance on the rotarod prior to falling off of the rod. The mice were tested three times per day with a minimal rest period of 5 min between trials and were tested for 3 consecutive days at 2, 5, 7, 9, 12, 14, 16, and 18 months of age. The longest latency of test day 3 was used to calculate performance. Open-field was used to measure locomotor activity, rearing, and exploration. The assay is performed in a plexiglass chamber (38 cm × 38 cm × 38 cm, L × W × H). Mice were tested at 2, 5, 7, 9, 12, 14, 16, and 18 months of age. Mice were placed into the center of the arena and allowed to freely explore for 10 min. Rearings were manually scored. Video recordings of each trial were analyzed using EthoVision XT (Noldus) software. Mouse locomotion was tracked by body center point. Center and peripheral (outer 1/3) regions of the arena were defined, and the time spent in each respective region was calculated. The footprint assay was used to analyze gait. Fore paws were painted with non-toxic red paint, and hind paws were painted with non-toxic blue paint. The mice were allowed to freely walk along a paper-covered runway that was enclosed by a darkened tunnel, leaving footprints on the runway. The hind-limb stride length was measured in millimeters (mm) for three consecutive steps, for at least 7 mice per genotype.

Tissue extractions for Western blot:

15–20 mg of tissue was homogenized in 250 μl of RIPA buffer with protease and phosphatase inhibitors using a probe homogenizer. Samples were centrifuged at 10,000g for 10 minutes at 4°C. Supernatant was collected and used as RIPA soluble fractions and the pellet was further processed to obtain the insoluble fraction. To collect the RIPA insoluble fractions, the pellets were resuspended with RIPA buffer and centrifuged again at 10,000g, and the supernatant was discarded. This pellet was rehomogenized with 250 μL Urea buffer [7 M urea, 2 M thiourea, 30 mM Tris pH 8.5, 4% 3-[(3-Cholamidopropyl) dimethylammonio]1-propanesulfonate (CHAPS, Sigma)]. The homogenate was centrifuged at 40,000g for 30 minutes. The resulting fraction was used as the RIPA insoluble fraction.

Western blotting analysis:

Samples were separated on NuPAGE 4–12% Bis-Tris gels (ThermoFisher Scientific) in 1X NuPAGE MOPS SDS Running Buffer (ThermoFisher Scientific). The proteins were then transferred onto 0.45 μM PVDF membrane (Merck Millipore Ltd.) in transfer buffer (90% 1X NuPAGE Transfer Buffer, 10% Methanol), then blocked with LiCor Odyssey Blocking Buffer (PBS, LiCor) and probed with primary antibody diluted in 1:1 blocking buffer in PBS or TBS. Blots were probed for MATR3 (Rabbit anti-MATR3-N, HPA036565, 1:1000, Sigma), TDP-43 (Rabbit anti-TDP-43-N, 10782–2-AP, 1:2000, Proteintech), pTDP43 (Mouse antiPhospho-TDP-43 (403/404), 66079–1-Ig, 1:500, Proteintech), and the loading control glyceraldehyde 3-phosphate dehydrogenase (GAPDH) (Rabbit anti-GAPDH mAb 14C10, #2118, 1:5000, Cell Signaling), then detected with fluorescent-labeled secondary antibodies (LiCor IRDye 800CW or IRDye 680RD Goat anti-mouse or Goat anti-rabbit, 1:5000) diluted in PBS or TBS, and imaged using the LiCor Odyssey CLx imager. Western blots were quantified using ImageJ.

Tissue preparation.

At sacrifice, mouse gastrocnemius muscle tissue was dissected, mounted on a piece of cork in 6% tragacanth gum, and flash frozen in a cooled bath (using liquid nitrogen, −150°C) of 2-methylbutane (Sigma). Flash frozen tissue was stored at −80°C. For gastrocnemius muscle staining, muscle tissue was cryosectioned into 14 μm slices.

Immunofluorescence of NMJs:

Gastrocnemius muscle from 18 mo mice was sectioned into 14 μm slices. Samples were washed twice for 5 min in 1X Tris Buffered Saline (TBS) + 0.3% Triton X-100 and then incubated in blocking solution (Super Block + 0.5% Triton X-100) for 1 hr at room temperature (RT). Samples were incubated in the primary antibody diluted in Super Block (Rabbit anti-Neurofilament L antibody, AB9568, EMD Millipore Corporation, 1:500) overnight at 4°C. The samples were rinsed twice for 5 min in 1X TBS + 0.3% Triton X-100 and then incubated in the secondary antibodies diluted in Super Block (Alexa Fluor 488 goat anti-rabbit IgG H&L, A11034, 1:500, Life Technologies Corporation); and α-Bungarotoxin-tetramethylrhodamine from *Bungarus multicinctus*, T0195, 1:500, Sigma) for 2 hr at RT. Samples were rinsed three times for 5 min in 1X PBS and then cover slipped using Fluoroshield.

Immunofluorescence on prepared gastrocnemius muscle sections:

Gastrocnemius muscle tissue of 24 mo mice were sectioned into 14 μm slices. The samples were washed for 5 min in 1X TBS + 0.3% Triton X-100 and then incubated in blocking solution (Super Block + 0.5% Triton X-100) for 1 hr at RT. Samples were incubated in the primary antibody diluted in Super Block (Rabbit anti-Laminin, ab11575, 1:1000, Abcam) overnight at 4°C. The samples were rinsed twice for 5 min in 1X TBS + 0.3% Triton X-100 and then incubated in the secondary antibody diluted in Super Block (Alexa Fluor 488 goat anti-rabbit IgG H&L, A11034, 1:1000, Life Technologies Corporation) for 2 hr at RT. Samples were rinsed three times for 5 min in 1X PBS and then cover slipped.

RNA Sequencing:

Sequencing libraries were generated from 150ng of RNA using SMARTer Stranded Total RNA Sample Prep Kit - HI Mammalian (Takara, 634874). Ribosomal RNA is depleted using Takara's ribogone Technology and single stranded DNA is generated with their template switching mechanism without the need for adapter ligation. cDNA fragments are purified using AMPure XP beads and then amplified using PCR. Libraries are characterized using D1000 high sensitivity screen tapes (Agilent) and quantified using qRT-PCR (Roche, KK4824P). Equimolar pools were generated, quantified (Roche, KK4824P), and sequenced on the Novaseq6000. The raw fastq files generated from SMARTer Stranded Total RNA-seq kit were trimmed 3 nt from both R1 and R2 using cutadapt. The index for the mapping is built using a reference genome - Genome Reference Consortium Mouse Build 38 and quantified using Salmon, a quasi-mapping algorithm to quantify transcript expression. The differential expression analysis was performed using DESEQ2 in R by incorporating the disease condition (WT and knock-in) in the design formula. Differentially expressed genes were selected based on the following criteria: p-value less than 0.05, a modulus of fold

change greater than 1.5 and a baseMean greater than 20. Heatmaps were generated with the r-log transformed values using pheatmap in R and volcano plots were generated using EnhancedVolcano in R with the abovementioned criteria.

Statistical Analysis:

Two-way ANOVA or One-way ANOVA with Bonferroni post hoc analysis was used to compare behavioral tests and quantification of pathological outputs. All error bars presented are SEM.

Results

Generation of MATR3 P154S knock-in mouse model

In collaboration with the Jackson Laboratory, we generated MATR3 P154S knock-in mice using CRISPR/Cas9. The P154S mutation was first identified in a single sporadic case (Johnson 2014). Sanger sequencing was performed to confirm the introduction of the mutation, which also introduced a silent mutation that removed a HaeIII restriction enzyme site (Figure 1A). Heterozygous mice ($Matr3^{P154S/+}$) were bred to establish colonies from 2 separate lines. In parallel, homozygous mice were found to be able breeders as well. In total, mice born from both lines were born at the expected Mendelian frequencies (Figure 1B), as observed in previous MATR3 knock-in mouse models [26,27]. Mice were allowed to age, and were assessed weekly for health and possible development of neuromuscular disease-like phenotypes (e.g. tremors, changes in splay). Both heterozygous and homozygous ($Matr3^{P154S/P154S}$) mice demonstrated normal lifespans. Weekly weight monitoring starting at weaning (21 days) demonstrated that both $Matr3^{P154S/P154S}$ and $Matr3^{P154S/+}$ did not differ in weight compared to wild-type ($Matr3^{+/+}$) in either mouse lines, nor between males or females (Figure 1C). These findings demonstrate that the P154S mutation does not significantly alter development, growth, or lifespan in either line.

MATR3 P154S mice lack behavioral or motor impairments

To test the effects of the MATR3 P154S mutation on neuromuscular function, mice were analyzed using various motor and behavioral tasks. Male and female mice from lines 1 and 2 were tested for motor function by rotarod starting at 2 months of age. Averaged together, there were no differences between $Matr3^{+/+}$, $Matr3^{P154S/+}$, and $Matr3^{P154S/P154S}$ mice up to 14 months of age (Figure 2A). Small, yet significant changes in female $Matr3^{P154S/+}$ and $Matr3^{P154S/P154S}$ performance were observed at 7 and 9 months of age in line 1, although these differences were not observed in line 2 and were likely due to variations within the small group size. (Supplemental Figure 1). Gait analysis was performed to measure changes in stance and stride in mice. At 14 months of age, no changes were observed in all measures including hind limb stride length (Figure 2B). In addition, mice were assayed using the open field test for 10 minutes per trial at 2, 7, and 14 months of age. There were no significant differences between groups at every time point (Figure 2C). Further, since MATR3 mutations have been associated with ALS-FTD, we also measured thigmotaxis to determine changes in anxiety-like behavior. Again, no differences were observed between groups at any time points (Figure 2D).

MATR3 P154S mice do not exhibit markers of muscle pathology

Previous transgenic and knock-in MATR3 models have demonstrated pathological changes in muscle tissue [26,28,29]. We measured average muscle fiber area in gastrocnemius cross sections at 8 months of age using confocal images of laminin immunostained sections. Quantification demonstrated that there were no significant differences between any of the groups (Figure 3A–B). Previously, MATR3 overexpression in transgenic mouse models demonstrated accumulation of matrin 3 protein in muscle tissue [28,29]. We found that matrin 3 localization was not altered in myocytes and found exclusively in nuclei in our P154S knock-in mice (Figure 3B). To determine if neuromuscular junction (NMJ) innervation was altered, we performed co-labeling of neurofilament to stain axonal tracks and α-bungarotoxin which labels acetylcholine receptors on muscle endplates. Quantification of innervated NMJs demonstrated that $Matr3^{P154S/+}$ and $Matr3^{P154S/P154S}$ showed no differences compared to $Matr3^{+/+}$ mice (Figure 3C). To test the effects of P154S mutations on protein expression levels, western blot analysis was performed on RIPA soluble 24-month-old gastrocnemius. Levels of matrin 3 protein were not impacted by genotype up to 24 months of age (Figure 3D).

MATR3 P154S does not induce neurodegenerative or inflammation

We next performed neuropathological analysis to determine the effects of the P154S mutation on neuropathologic markers such as neuroinflammation, protein aggregation, and neurodegeneration. Matrin 3 protein is known to aggregate in neurons in postmortem tissue from patients with MATR3 mutations as well as in sporadic ALS [7,22,30]. We performed immunofluorescence (IF) for Matrin 3 in lumbar spinal cord of 18-month-old mice and found that Matrin 3 localization was not altered in $Matr3^{P154S/+}$ or $Matr3^{P154S/P154S}$ compared to controls (Figure 4A). Matrin 3 protein was located only in nuclei throughout the spinal cord. This finding is in line with *in vitro* and *in vivo* findings that mutations do not drastically alter the cellular distribution of matrin 3 [27,31]. In addition, we performed Western blot analysis on soluble and insoluble fractions from spinal cord of 24-month-old mice. We found that matrin 3 levels were not altered at 24 months of age in any genotypes in either the soluble or insoluble fractions (Figure 4B). As loss of spinal motor neurons (MN) is a hallmark feature of ALS, we measured the impact of the MATR3 P154S variant on MN death in the spinal cord. We performed IF staining for choline acetyltransferase (ChAT) and quantified the number of MNs in the ventral horn of the lumbar spinal cord. Analysis demonstrated that MNs number was not altered in either $Matr3^{P154S/+}$ or $Matr3^{P154S/P154S}$ mice (Figure 4C). In addition, we assessed neuroinflammation via Iba-1 via IHC. We found that staining intensity was not changed between genotypes, and these findings were confirmed using western blot analysis for Iba-1 which showed no difference in Iba-1expression levels in spinal cord extracts. Finally, bulk RNAseq analysis was performed on spinal cords collected from 24-month-old wild-type and $Matr3^{P154S/P154S}$ mice. Analysis demonstrated few genes were differentially expressed in homozygous mice compared to wild-type (Supplementary Figure 2A–B).

DISCUSSION:

To date, 13 missense mutations in MATR3 have been identified to associate with ALS and distal myopathy. The MATR3 P154S mutation was originally reported in a sporadic patient following sequencing of 96 British ALS cases [7]. Subsequent studies aimed at determining the roles of MATR3 mutations in neurodegeneration demonstrated that the P154S mutation did indeed exert functional changes. For example, overexpression of MATR3 P154S in primary rodent cortical neurons demonstrated significantly increased toxicity compared to overexpressing wild-type MATR3 [25], and was comparable in toxicity to other MATR3 mutations tested such as S85C and F115C. Further, the P154S mutation was also associated with altered interactions with protein members of the Transcription and Export (TREX) and changes in global RNA transport [23] compared to wild-type matrin 3. These functional changes supported our hypothesis that expression of MATR3 P154S *in vivo* would produce motor neuron disease and myopathy-like phenotype. Here, we find that knock-in of the ALS-linked MATR3 P154S mutation is not sufficient to produce an ALS- or myopathy-like phenotype in heterozygous nor homozygous genotypes. Observations from two independently generated lines demonstrated no phenotypic or functional changes in $Matr3^{P154S/+}$ and $Matr3^{P154S/P154S}$ mice for up to 24 months of age when compared to wild-type littermates. Lack of phenotype extended into the pathological and biochemical characterization of the mutant mouse tissues. Analyses of muscle tissues showed no signs of atrophy or pathological hallmarks of myopathy such as centralized nuclei. Likewise, we found no evidence of MN loss, matrin 3 pathology, or neuroinflammation within the spinal cords of MATR3 P154S mice. These findings contrast with most available matrin 3 mutant mice that have been presented in the literature.

The first mouse models of Matrin 3 used overexpression approaches to understand the role of matrin 3 in disease. Wild-type and MATR3 F115C mutation overexpression models displayed dramatic pathology in the muscle. Overexpression resulted in muscle atrophy, muscle vacuolization, and matrin 3 protein mislocalization [29]. Similar results were obtained in a separate mouse model using adeno-associated viral vectors to increase wild-type or MATR3 S85C mutant protein [28]. When overexpressed in the tibialis anterior muscle, wild-type and MATR3 S85C mutant protein induced drastic muscle atrophy and degeneration. Moreover, transgenic mice overexpressing wild-type and MATR3 S85C in the central nervous system and muscle demonstrated pathology in both sets of tissues. Both wild-type and S85C transgenic mouse models exhibited muscle degeneration, motor neuron loss and neuroinflammation [28]. Together, these studies demonstrate how increased matrin 3 levels can produced proteinopathy in the CNS and muscle tissues. However, these models present a caveat that perhaps the pathology observed in these models is due to transgene overexpression, and not reflective of the human disease state that exhibits endogenous gene expression. Recently, knock-in mouse models have been generated to address this possibility. An S85C mouse knock-in mouse model was produced that did not exhibit increased levels of matrin 3 [26]. However, homozygous S85C mutant mice did exhibit motor impairments, muscle atrophy, Purkinje cell loss, and neuroinflammation [26]. In contrast, another knock-in mouse model expressing the MATR3 F115C mutation lacked any phenotype or neuropathology [27]. This suggest that MATR3 mutations may vary in

their pathogenicity. It is important to note, however, that since the original report identifying F115C as a causative mutation, re-analysis of the family found an intronic mutation in KIF5A [32]. Thus, the MATR3 F115C mutation may not represent a disease causative mutation.

We hypothesized that expressing the MATR3 P154S mutation under the control of endogenous regulatory elements would produce an ALS and/or myopathy phenotype. The lack of phenotype in our knock-in mice diverges from overexpression models and the S85C knock-in mouse models. Instead, it mirrors the findings from the MATR3 F115C knock-in mouse model. Based on these findings, we postulate the MATR3 P154S variant is not causal for disease. However, that conclusion requires further genomic analysis. It is possible that the P154S mutation is not deleterious enough to produce a phenotype in mice within the 24 months we observed. To illustrate that point, knock-in mouse models using ALS-associated mutations in TDP-43 do not always produce a neurodegenerative phenotype even in homozygous mice [33,34]. Another secondary stressor may be required to induce a phenotype and pathology, suggesting that the MATR3 P154S variant increases susceptibility to neurodegeneration. Further studies are required to test this possibility, but our results indicate that the MATR3 P154S mutation does not independently induce a motor phenotype or pathology in mice.

Supplementary Material

Refer to Web version on PubMed Central for supplementary material.

Acknowledgments

We thank The Jackson Laboratory for support to generate the MATR3 P154S knock-in mouse model. This study was also supported by the Barrow Neurological Foundation, the Fein Family Foundation, and NIH grant R21 NS116385 awarded to DXM and RB.

References

[1]. Chen JJ, Overview of current and emerging therapies for amytrophic lateral sclerosis, Am. J. Manag. Care 26 (2020) S191–S197. 10.37765/ajmc.2020.88483. [PubMed: 32840332]

[2]. Paganoni S, Macklin EA, Hendrix S, Berry JD, Elliott MA, Maiser S, Karam C, Caress JB, Owegi MA, Quick A, Wymer J, Goutman SA, Heitzman D, Heiman-Patterson T, Jackson CE, Quinn C, Rothstein JD, Kasarskis EJ, Katz J, Jenkins L, Ladha S, Miller TM, Scelsa SN, Vu TH, Fournier CN, Glass JD, Johnson KM, Swenson A, Goyal NA, Pattee GL, Andres PL, Babu S, Chase M, Dagostino D, Dickson SP, Ellison N, Hall M, Hendrix K, Kittle G, McGovern M, Ostrow J, Pothier L, Randall R, Shefner JM, Sherman AV, Tustison E, Vigneswaran P, Walker J, Yu H, Chan J, Wittes J, Cohen J, Klee J, Leslie K, Tanzi RE, Gilbert W, Yeramian PD, Schoenfeld D, Cudkowicz ME, Trial of Sodium Phenylbutyrate–Taurursodiol for Amyotrophic Lateral Sclerosis, N. Engl. J. Med 383 (2020) 919–930. 10.1056/NEJMoa1916945. [PubMed: 32877582]

[3]. Mejzini R, Flynn LL, Pitout IL, Fletcher S, Wilton SD, Akkari PA, ALS Genetics, Mechanisms, and Therapeutics: Where Are We Now?, Front. Neurosci 13 (2019) 1310. 10.3389/fnins.2019.01310. [PubMed: 31866818]

[4]. Feit H, Silbergleit A, Schneider LB, Gutierrez JA, Fitoussi RP, Réyès C, Rouleau GA, Brais B, Jackson CE, Beckmann JS, Seboun E, Vocal cord and pharyngeal weakness with autosomal dominant distal myopathy: clinical description and gene localization to 5q31, Am. J. Hum. Genet 63 (1998) 1732–1742. 10.1086/302166. [PubMed: 9837826]

[5]. Senderek J, Garvey SM, Krieger M, Guergueltcheva V, Urtizberea A, Roos A, Elbracht M, Stendel C, Tournev I, Mihailova V, Feit H, Tramonte J, Hedera P, Crooks K, Bergmann C, Rudnik-Schöneborn S, Zerres K, Lochmüller H, Seboun E, Weis J, Beckmann JS, Hauser MA, Jackson CE, Autosomal-Dominant Distal Myopathy Associated with a Recurrent Missense Mutation in the Gene Encoding the Nuclear Matrix Protein, Matrin 3, Am. J. Hum. Genet 84 (2009) 511–518. 10.1016/j.ajhg.2009.03.006. [PubMed: 19344878]

[6]. Müller TJ, Kraya T, Stoltenburg-Didinger G, Hanisch F, Kornhuber M, Stoevesandt D, Senderek J, Weis J, Baum P, Deschauer M, Zierz S, Phenotype of matrin-3-related distal myopathy in 16 German patients, Ann. Neurol 76 (2014) 669–680. 10.1002/ana.24255. [PubMed: 25154462]

[7]. Johnson JO, Pioro EP, Boehringer A, Chia R, Feit H, Renton AE, Pliner HA, Abramzon Y, Marangi G, Winborn BJ, Gibbs JR, Nalls MA, Morgan S, Shoai M, Hardy J, Pittman A, Orrell RW, Malaspina A, Sidle KC, Fratta P, Harms MB, Baloh RH, Pestronk A, Weihl CC, Rogaeva E, Zinman L, Drory VE, Borghero G, Mora G, Calvo JD Rothstein, ITALSGEN, C. Drepper, M. Sendtner, A.B. Singleton, J.P. Taylor, M.R. Cookson, G. Restagno, M. Sabatelli, R. Bowser, A. Chiò, B.J. Traynor, Mutations in the Matrin 3 gene cause familial amyotrophic lateral sclerosis, Nat. Neurosci 17 (2014) 664–666. 10.1038/nn.3688. [PubMed: 24686783]

[8]. Marangi G, Lattante S, Doronzio PN, Conte A, Tasca G, Monforte M, Patanella AK, Bisogni G, Meleo E, La Spada S, Zollino M, Sabatelli M, Matrin 3 variants are frequent in Italian ALS patients, Neurobiol. Aging 49 (2017) 218.e1–218.e7. 10.1016/j.neurobiolaging.2016.09.023.

[9]. Xu L, Li J, Tang L, Zhang N, Fan D, MATR3 mutation analysis in a Chinese cohort with sporadic amyotrophic lateral sclerosis, Neurobiol. Aging 38 (2016) 218.e3–218.e4. 10.1016/j.neurobiolaging.2015.11.023.

[10]. Lin K-P, Tsai P-C, Liao Y-C, Chen W-T, Tsai C-P, Soong B-W, Lee Y-C, Mutational analysis of MATR3 in Taiwanese patients with amyotrophic lateral sclerosis, Neurobiol. Aging 36 (2015) 2005.e1–4. 10.1016/j.neurobiolaging.2015.02.008.

[11]. Leblond CS, Gan-Or Z, Spiegelman D, Laurent SB, Szuto A, Hodgkinson A, Dionne-Laporte A, Provencher P, de Carvalho M, Orrù S, Brunet D, Bouchard J-P, Awadalla P, Dupré N, Dion PA, Rouleau GA, Replication study of MATR3 in familial and sporadic amyotrophic lateral sclerosis, Neurobiol. Aging 37 (2016) 209.e17–209.e21. 10.1016/j.neurobiolaging.2015.09.013.

[12]. Zhang Z, Carmichael GG, The fate of dsRNA in the nucleus: a p54(nrb)-containing complex mediates the nuclear retention of promiscuously A-to-I edited RNAs, Cell 106 (2001) 465–475. [PubMed: 11525732]

[13]. Salton M, Lerenthal Y, Wang S-Y, Chen DJ, Shiloh Y, Involvement of Matrin 3 and SFPQ/NONO in the DNA damage response, Cell Cycle Georget. Tex 9 (2010) 1568–1576. 10.4161/cc.9.8.11298.

[14]. Salton M, Elkon R, Borodina T, Davydov A, Yaspo M-L, Halperin E, Shiloh Y, Matrin 3 binds and stabilizes mRNA, PloS One 6 (2011) e23882. 10.1371/journal.pone.0023882. [PubMed: 21858232]

[15]. Gallego-Iradi MC, Clare AM, Brown HH, Janus C, Lewis J, Borchelt DR, Subcellular Localization of Matrin 3 Containing Mutations Associated with ALS and Distal Myopathy, PloS One 10 (2015) e0142144. 10.1371/journal.pone.0142144. [PubMed: 26528920]

[16]. Iradi MCG, Triplett JC, Thomas JD, Davila R, Crown AM, Brown H, Lewis J, Swanson MS, Xu G, Rodriguez-Lebron E, Borchelt DR, Characterization of gene regulation and protein interaction networks for Matrin 3 encoding mutations linked to amyotrophic lateral sclerosis and myopathy, Sci. Rep 8 (2018) 4049. 10.1038/s41598018-21371-4. [PubMed: 29511296]

[17]. Boehringer A, Garcia-Mansfield K, Singh G, Bakkar N, Pirrotte P, Bowser R, ALS Associated Mutations in Matrin 3 Alter Protein-Protein Interactions and Impede mRNA Nuclear Export, Sci. Rep 7 (2017) 14529. 10.1038/s41598-017-14924-6. [PubMed: 29109432]

[18]. Johnson JO, Pioro EP, Boehringer A, Chia R, Feit H, Renton AE, Pliner HA, Abramzon Y, Marangi G, Winborn BJ, Gibbs JR, Nalls MA, Morgan S, Shoai M, Hardy J, Pittman A, Orrell RW, Malaspina A, Sidle KC, Fratta P, Harms MB, Baloh RH, Pestronk A, Weihl CC, Rogaeva E, Zinman L, Drory VE, Borghero G, Mora G, Calvo JD Rothstein, ITALSGEN, C. Drepper, M. Sendtner, A.B. Singleton, J.P. Taylor, M.R. Cookson, G. Restagno, M. Sabatelli, R. Bowser, A. Chiò, B.J. Traynor, Mutations in the Matrin 3 gene cause familial amyotrophic lateral sclerosis, Nat. Neurosci 17 (2014) 664–666. 10.1038/nn.3688. [PubMed: 24686783]

[19]. Kamelgarn M, Chen J, Kuang L, Arenas A, Zhai J, Zhu H, Gal J, Proteomic analysis of FUS interacting proteins provides insights into FUS function and its role in ALS, Biochim. Biophys. Acta 1862 (2016) 2004–2014. 10.1016/j.bbadis.2016.07.015. [PubMed: 27460707]

[20]. Yamaguchi A, Takanashi K, FUS interacts with nuclear matrix-associated protein SAFB1 as well as Matrin3 to regulate splicing and ligand-mediated transcription, Sci. Rep 6 (2016). 10.1038/srep35195.

[21]. Dreser A, Vollrath JT, Sechi A, Johann S, Roos A, Yamoah A, Katona I, Bohlega S, Wiemuth D, Tian Y, Schmidt A, Vervoorts J, Dohmen M, Beyer C, Anink J, Aronica E, Troost D, Weis J, Goswami A, The ALS-linked E102Q mutation in Sigma receptor-1 leads to ER stress-mediated defects in protein homeostasis and dysregulation of RNA-binding proteins, Cell Death Differ 24 (2017) 1655–1671. 10.1038/cdd.2017.88. [PubMed: 28622300]

[22]. Tada M, Doi H, Koyano S, Kubota S, Fukai R, Hashiguchi S, Hayashi N, Kawamoto Y, Kunii M, Tanaka K, Takahashi K, Ogawa Y, Iwata R, Yamanaka S, Takeuchi H, Tanaka F, Matrin 3 Is a Component of Neuronal Cytoplasmic Inclusions of Motor Neurons in Sporadic Amyotrophic Lateral Sclerosis, Am. J. Pathol 188 (2018) 507–514. 10.1016/j.ajpath.2017.10.007. [PubMed: 29128563]

[23]. Boehringer A, Garcia-Mansfield K, Singh G, Bakkar N, Pirrotte P, Bowser R, ALS Associated Mutations in Matrin 3 Alter Protein-Protein Interactions and Impede mRNA Nuclear Export, Sci. Rep 7 (2017) 14529. 10.1038/s41598-017-14924-6. [PubMed: 29109432]

[24]. Sprunger ML, Lee K, Sohn BS, Jackrel ME, Molecular determinants and modifiers of Matrin-3 toxicity, condensate dynamics, and droplet morphology, IScience 25 (2022) 103900. 10.1016/j.isci.2022.103900. [PubMed: 35252808]

[25]. Malik AM, Miguez RA, Li X, Ho Y-S, Feldman EL, Barmada SJ, Matrin 3-dependent neurotoxicity is modified by nucleic acid binding and nucleocytoplasmic localization, ELife 7 (2018) e35977. 10.7554/eLife.35977. [PubMed: 30015619]

[26]. Kao CS, van Bruggen R, Kim JR, Chen XXL, Chan C, Lee J, Cho WI, Zhao M, Arndt C, Maksimovic K, Khan M, Tan Q, Wilson MD, Park J, Selective neuronal degeneration in MATR3 S85C knock-in mouse model of early-stage ALS, Nat. Commun 11 (2020) 5304. 10.1038/s41467-020-18949-w. [PubMed: 33082323]

[27]. van Bruggen R, Maksimovic K, You J, Tran DD, Lee HJ, Khan M, Kao CS, Kim JR, Cho W, Chen XXL, Park J, MATR3 F115C knock-in mice do not exhibit motor defects or neuropathological features of ALS, Biochem. Biophys. Res. Commun 568 (2021) 48–54. 10.1016/j.bbrc.2021.06.052. [PubMed: 34182213]

[28]. Zhang X, Yamashita S, Hara K, Doki T, Tawara N, Ikeda T, Misumi Y, Zhang Z, Matsuo Y, Nagai M, Kurashige T, Maruyama H, Ando Y, A mutant MATR3 mouse model to explain multisystem proteinopathy, J. Pathol 249 (2019) 182–192. 10.1002/path.5289. [PubMed: 31056746]

[29]. Moloney C, Rayaprolu S, Howard J, Fromholt S, Brown H, Collins M, Cabrera M, Duffy C, Siemienski Z, Miller D, Borchelt DR, Lewis J, Analysis of spinal and muscle pathology in transgenic mice overexpressing wild-type and ALS-linked mutant MATR3, Acta Neuropathol. Commun 6 (2018) 137. 10.1186/s40478-018-0631-0. [PubMed: 30563574]

[30]. Ramesh N, Kour S, Anderson EN, Rajasundaram D, Pandey UB, RNA-recognition motif in Matrin-3 mediates neurodegeneration through interaction with hnRNPM, Acta Neuropathol. Commun 8 (2020) 138. 10.1186/s40478-020-01021-5. [PubMed: 32811564]

[31]. Gallego-Iradi MC, Strunk H, Crown AM, Davila R, Brown H, Rodriguez-Lebron E, Borchelt DR, N-terminal sequences in matrin 3 mediate phase separation into droplet-like structures that recruit TDP43 variants lacking RNA binding elements, Lab. Invest 99 (2019) 1030–1040. 10.1038/s41374-019-0260-7. [PubMed: 31019288]

[32]. Saez-Atienzar S, Dalgard CL, Ding J, Chiò A, Alba C, Hupalo DN, Wilkerson MD, Bowser R, Pioro EP, Bedlack R, Traynor BJ, Identification of a pathogenic intronic KIF5A mutation in an ALS-FTD kindred, Neurology 95 (2020) 1015–1018. 10.1212/WNL.0000000000011064. [PubMed: 33077544]

[33]. Watanabe S, Oiwa K, Murata Y, Komine O, Sobue A, Endo F, Takahashi E, Yamanaka K, ALS-linked TDP-43M337V knock-in mice exhibit splicing deregulation without neurodegeneration, Mol. Brain 13 (2020) 8. 10.1186/s13041-020-0550-4. [PubMed: 31959210]

[34]. Huang S-L, Wu L-S, Lee M, Chang C-W, Cheng W-C, Fang Y-S, Chen Y-R, Cheng P-L, Shen C-KJ, A robust TDP-43 knock-in mouse model of ALS, Acta Neuropathol. Commun 8 (2020) 3. 10.1186/s40478-020-0881-5. [PubMed: 31964415]

Highlights

- P154S matrin 3 mutation does not cause pathology in novel knock-in mouse model.
- Novel matrin 3 knock-in mouse model does not produce neurodegeneration or myopathy phenotype.
- Lack of neurodegenerative phenotype in P154S matrin 3 knock-in mouse model.
- Behavioral and pathological characterization of novel P154S Matrin 3 mutant mouse model.

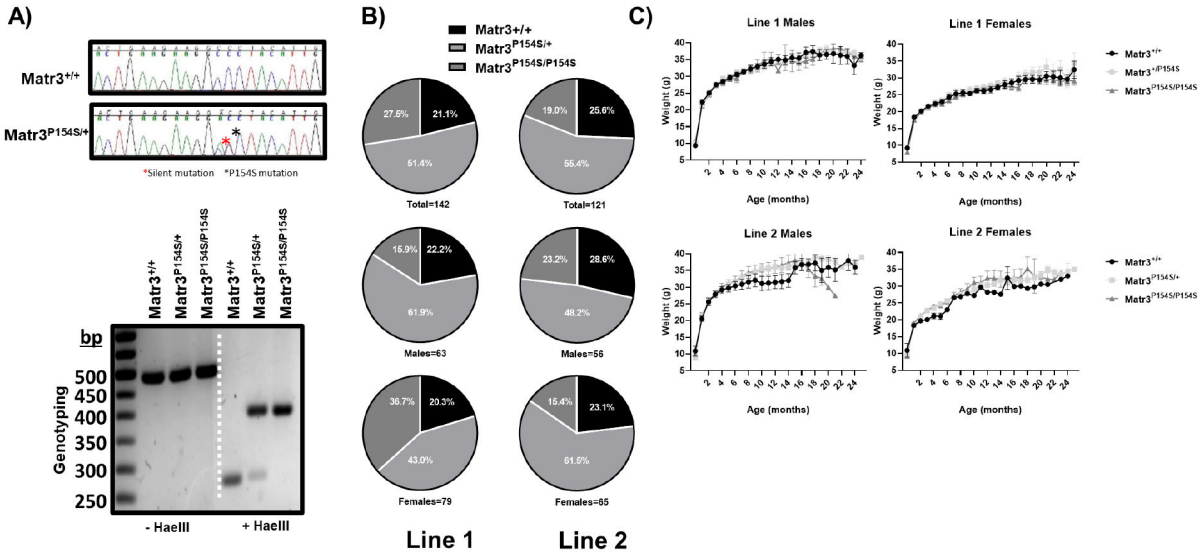

Figure 1: Generation of MATR3 P154S knock-in mice:

A) Heterozygous mice were generated by Jackson Lab and validated via Sanger sequencing (top). The presence of a silent mutation removed a restriction site that could be used to validate genotypes via PCR (bottom). Homozygous mice completely lacked this restriction site. B) Mutant MATR3 mice were produced at the expected Mendelian ratios in both lines 1 and 2, with no significant differences observed (chi squared test for goodness of fit). C) Longitudinal tracking of average mouse weights demonstrate the P154S mutation did not cause changes in either males or females ($p<0.05$, Two-Way ANOVA) (n=18–20 per group).

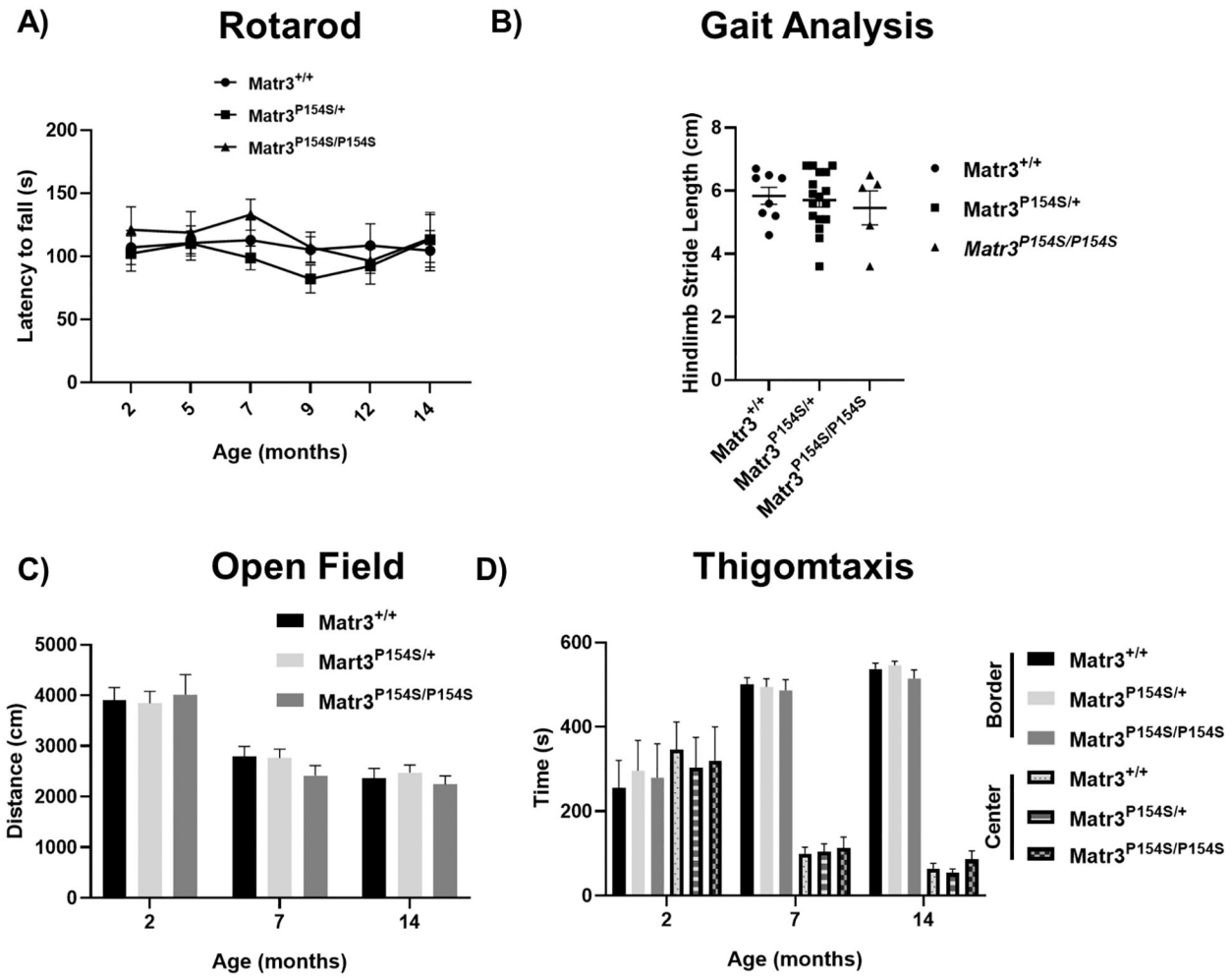

Figure 2: Behavioral Analysis of MATR3 P154S knock-in mice demonstrates P154S mutation does not cause motor impairments.

A) Longitudinal rotarod analysis demonstrated that MATR3$^{P154S/+}$ and MATR3$^{P154S/P154S}$ mice do not demonstrate declines with age or significant changes from WT performance. B) Footprint analysis demonstrated the average hindlimb stride length was not changed in 18-month-old MATR3$^{P154S/+}$ or MATR3$^{P154S/P154S}$ mice. C) Open-Field Task (left) was used to measure locomotor activity, and found that distance moved during a 10minute trial was not significantly different in MATR3$^{P154S/+}$ or MATR3$^{P154S/P154S}$ compared to WT mice. Thigmotaxis (right) was measured with the open field, and likewise demonstrated no differences between genotypes. ($p<0.05$, Two-Way repeated measures ANOVA) (n=10–15 per group).

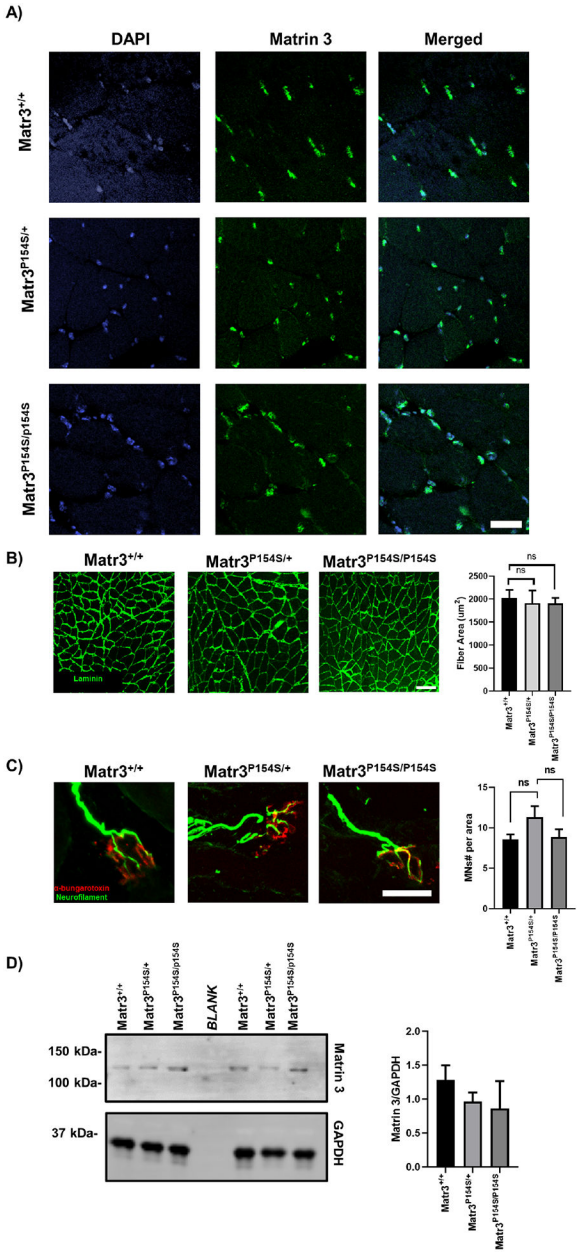

Figure 3: MATR3 P154S knock-in does not produce myopathology at 24 months-of-age.

A) Matrin 3 IF of gastrocnemius muscle demonstrates no changes of nuclear localization of Matrin 3 in MATR3$^{P154S/+}$ or MATR3$^{P154S/P154S}$. Scale bar=30 μm. B) Laminin IF of gastrocnemius muscle; (Graph) Quantification of fiber diameter demonstrates no changes between genotypes. Scale bar=100 μm. C) Neuromuscular junction analysis; α-bungarotoxin (red) labeling and neurofilament (green) co-localization in gastrocnemius muscle; (Graph) quantification of innervated NMJs. Scale bar=20μm. D) Western blot analysis of Matrin 3 from RIPA soluble fraction (left) and insoluble fraction (right) from gastrocnemius (n=3/genotype). One-way ANOVA was performed on quantifications.

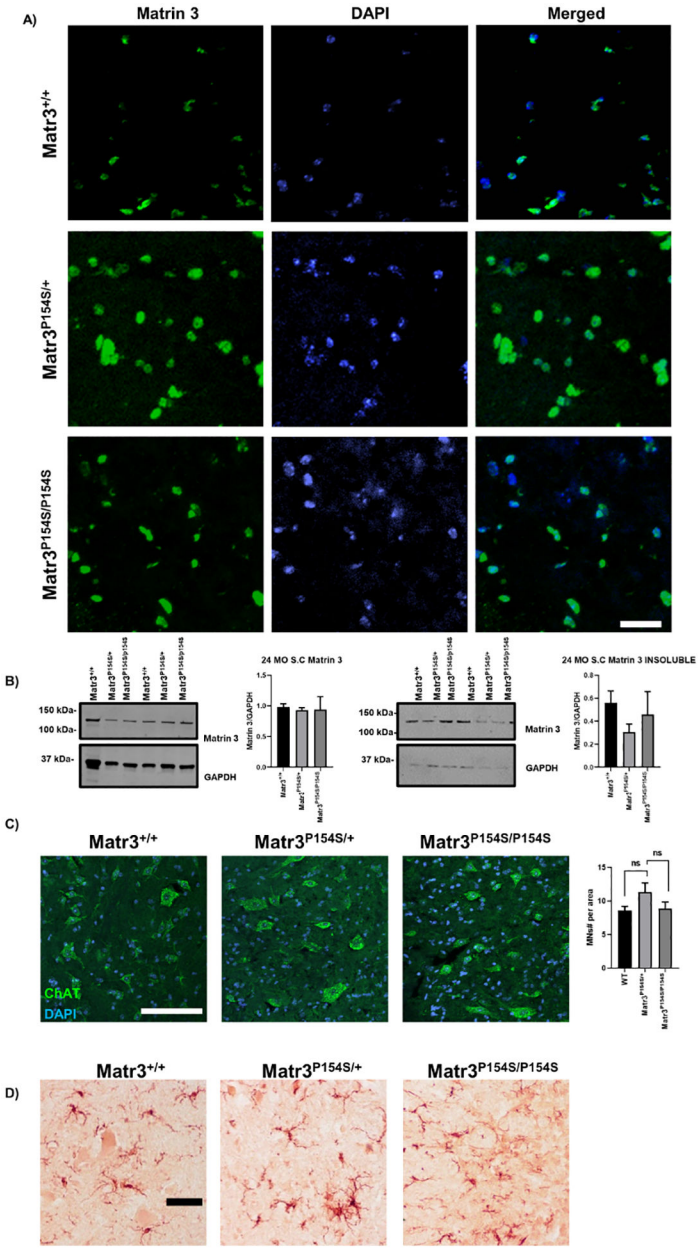

Figure 4: MATR3 P154S knock-in does not produce neuropathology at 18 months-of-age.

A) Representative images of Matrin 3 immunofluorescence (green) from lumbar spinal cord show nuclear localization. Scale bar= 25 μm. B) Western blot analysis of Matrin 3 from RIPA soluble fraction (left) and insoluble fraction (right) from spinal cord (n=3–4/genotype). C) Representative images of ChAT IF in lumbar spinal cord (Graph) quantification of motor neuron number in ventral horn. Scale bar=100 μm D) Iba-1 IHC in lumbar spinal cord. Scale bar=100μm.